scientific reports

Check for updates

OPEN

The preclinical study of biocompatibility of tyrosine polycarbonate bioresorbable scaffold in small caliber porcine peripheral arteries

Mateusz Kachel[1,2], Pedro H. C. Melo[1], Yanping Cheng[1], Gerard B. Conditt[1], Danielle Gram[3], Jeffrey Anderson[3], Serge D. Rousselle[4], Sahil A. Parikh[1,5], Juan F. Granada[1] & Grzegorz L. Kaluza[1]✉

Drug-eluting resorbable scaffolds (DRS) are conceptually attractive for treatment of peripheral arterial disease, particularly below-the-knee. MOTIV is a peripheral variant of REVA Medical's well-established, radiopaque tyrosine-polycarbonate (Tyrocore) sirolimus-eluting DRS. The purpose of this study was to provide imaging and histopathologic data on vascular response to MOTIV in porcine peripheral arteries. MOTIV scaffolds (3.0 or 3.5 × 12/24/36/48/60 mm) were implanted in 20 internal iliac arteries of 9 Yorkshire swine. At 30 and 90 days, vascular stenosis, strut coverage, and strut apposition were characterized using optical coherence tomography. Scaffold structure and vascular healing were assessed by histopathology and scanning electron microscopy. At termination, all vessels remained patent. The average neointimal thickness was 0.22 ± 0.05 mm in Group 1 (30 days) and 0.18 ± 0.10 mm in Group 2 (90 days); the percent area stenosis was 28 ± 6% and 24 ± 11%, respectively. All struts were fully covered by neointima. No malapposition, stent fracture or late strut discontinuity was observed. Adequate vessel wall healing at both time points was characterized by a typically fully mature neointima and complete reendothelialization at all sites. No unresorbed luminal thrombus was observed. The inflammation scores were low for all vessels on both time points, except for one animal. The average inflammation (excluding multinucleated giant cells [MNGCs]) was 0.6 (MNGCs score was 0.9) for the stented vessel segments at 30 days and 0.8 (MNGCs score of 1.0) at 90 days. Implantation of the MOTIV up to 60 mm long in small-caliber peripheral arteries of swine resulted in 100% patency rate and adequate vascular healing at 30-day and 90-day timepoints. The Tyrocore-based DRS retained the necessary structural integrity throughout the course of the study and confirmed their favorable biocompatibility in small-caliber porcine peripheral arteries.

Keywords Below-the-knee, Bioresorbable scaffolds, Animal model, Peripheral arterial disease, Chronic limb threatening ischemia, Tyrocore

Abbreviations

PAD	Peripheral arterial disease
CLTI	Chronic limb threatening ischemia
BTK	Below-the-knee
DRS	Drug–eluting resorbable scaffold
PLLA	Poly–L–lactic acid
SEM	Scanning electron microscopy
MLD	Minimal lumen diameter
RVD	Reference vessel diameter

[1]Skirball Center for Innovation, Cardiovascular Research Foundation, Orangeburg, NY, USA. [2]AHP Center for Cardiovascular Research and Development, Katowice, Poland. [3]REVA Medical, San Diego, CA, USA. [4]StageBio, Mt. Jackson, VA, USA. [5]Columbia University Medical Center, New York, NY, USA. ✉email: gkaluza@crf.org

NIT	Neointimal thickness
ROUS	Ratio of uncovered struts

Peripheral arterial disease (PAD) remains a major challenge for healthcare systems across the globe with over 200 million people affected worldwide[1]. The number is set to grow further due to the aging population. PAD's most severe manifestation, chronic limb-threatening ischemia (CLTI), will potentially occur in up to 11% of patients requiring urgent intervention to prevent imminent limb loss[2].

The advances in techniques and technology facilitated the increased use of endovascular methods over bypass surgery[3]. The drug-eluting stents (DESs) proved to be superior to balloon angioplasty and bare-metal stents in preserving patency for up to 12 months in infra-popliteal lesions[4,5]. Although the acute results have substantially improved, the restenosis rate remains high in the long term, particularly in the below-the-knee (BTK) patients' subset[6]. Furthermore, the presence of a permanent metallic scaffold implicates several significant limitations. The rigid implant affects the vessel by impairing the vasomotor tone, inducing endothelial dysfunction, chronic inflammation, and consequently excessive late lumen loss[7,8]. Furthermore, the distinctive anatomy of the infra-popliteal region creates concern over excessive external force leading to stent compression and infrequently fracture[9]. Metallic stent placement in the BTK artery may preclude future bypass surgery underscoring the need for a well-weighted decision[10].

The drug-eluting resorbable scaffolds (DRS) were created to overcome the limitations of traditional devices. The intriguing "leave nothing behind" concept sparked an interest in the initial generation of PLLA-made devices in the coronary territory. The rapid rise of DRS in coronary application was suddenly halted by reports of increased rates of stent thrombosis with the leading PLLA-based scaffold as compared with contemporary DES[11,12]. As a result, all DRS in development at the time have been prematurely stigmatized with a class-failure label, even though many were technologically different, and some used entirely different materials such as metallic alloys or tyrosine polycarbonate (Tyrocore)[13]. Although the concerns about negative long-term safety outcomes proved largely unfounded with these non-PLLA based coronary scaffolds[14,15], the use of DRS in coronary applications remains very limited. However, the favorable potential of DRS in BTK arterial disease has been recognized[16–19]. The recently presented results of LIFE BTK confirmed that DRS are not just an interesting theoretical concept, but a viable treatment option in peripheral arteries, showcasing their superiority in terms of efficacy, while retaining a similar safety profile to that of balloon angioplasty[18]. The favorable outcomes translated into the recent FDA approval that was granted to Espirit BTK (Abbott) for the treatment of below-the-knee lesions. To that end, we present preclinical results of novel MOTIV bioresorbable scaffolds for the treatment of BTK lesions.

Methods

The study hypothesized that the Tyrocore-based scaffold validated in coronary clinical use retains its early integrity and biocompatibility in a more biomechanically demanding peripheral vasculature, even at longer lengths, previously not evaluated.

Study device

The MOTIV scaffold (REVA Medical, Inc. San Diego, CA) is a balloon-expandable, sirolimus-eluting, open-cell scaffold design (Fig. 1) made from Tyrocore, a novel polycarbonate polymer comprised of analogs of the natural amino acid tyrosine (desaminotyrosine) and biocompatible hydroxy- esters (e.g., lactic acid). In comparison to previously published properties of poly-L-lactic acid (PLLA), Tyrocore features higher ultimate tensile strength (100–110 MPa vs. 50–70 MPa for PLLA) and elongation (ductility, 150–200% vs. 2–10% for PLLA)[20]. The radiopacity of the scaffold structure is equivalent to currently marketed metallic stents. After implantation, the scaffold elutes a substantial portion of sirolimus within 30 days. The coating used for the drug elution is the same polymer that is used to make the scaffold platform, applied abluminally to elute sirolimus at 1.97 $\mu g/mm^2$ dose density.

Tyrocore polymer features a steady resorption profile. One year after implantation, the vessel becomes uncaged, and the material fully resorbs within 4 years. The following MOTIV stent sizes (strut thickness) and lengths were used in the study to allow for testing of both short and long scaffolds: 2.5 mm (95 µm) x 24 mm; 3.0 mm (105 µm) x 12, 18, 24, 36 and 48 mm; 3.5 mm (115 µm) x12, 18, 24, 36, 48 and 60 mm.

Experimental model

The study was approved by the Institutional Animal Care and Use Committee and conducted in accordance with the Animal Welfare Act and the Guide for the Care and Use of Laboratory Animals (National Research Council, National Institutes of Health publication no. 85 – 23, revised 1996) at U.S. Department of Agriculture-licensed, Association for the Assessment and Accreditation of Laboratory Animal Care International-accredited animal research facility.

Accordance statement

The study is reported in accordance with ARRIVE guidelines.

Experimental procedure

A total of nine (9) Yorkshire swine were enrolled in the study. All animals were sourced from an accredited vendor (Manthei Hog Farm; 23130 112th St NW, Elk River, MN 55330). Three (3) animals were implanted with the test article in naïve peripheral arteries and survived to 30 days (Group 1), and six (6) animals survived to 90 days (Group 2). All procedures were performed under general anesthesia maintained with the use of isoflurane in 100% O_2 (inhalation; 0–5%) and propofol (IV.; 2–8 mg/kg). The exact distribution of animals and scaffolds

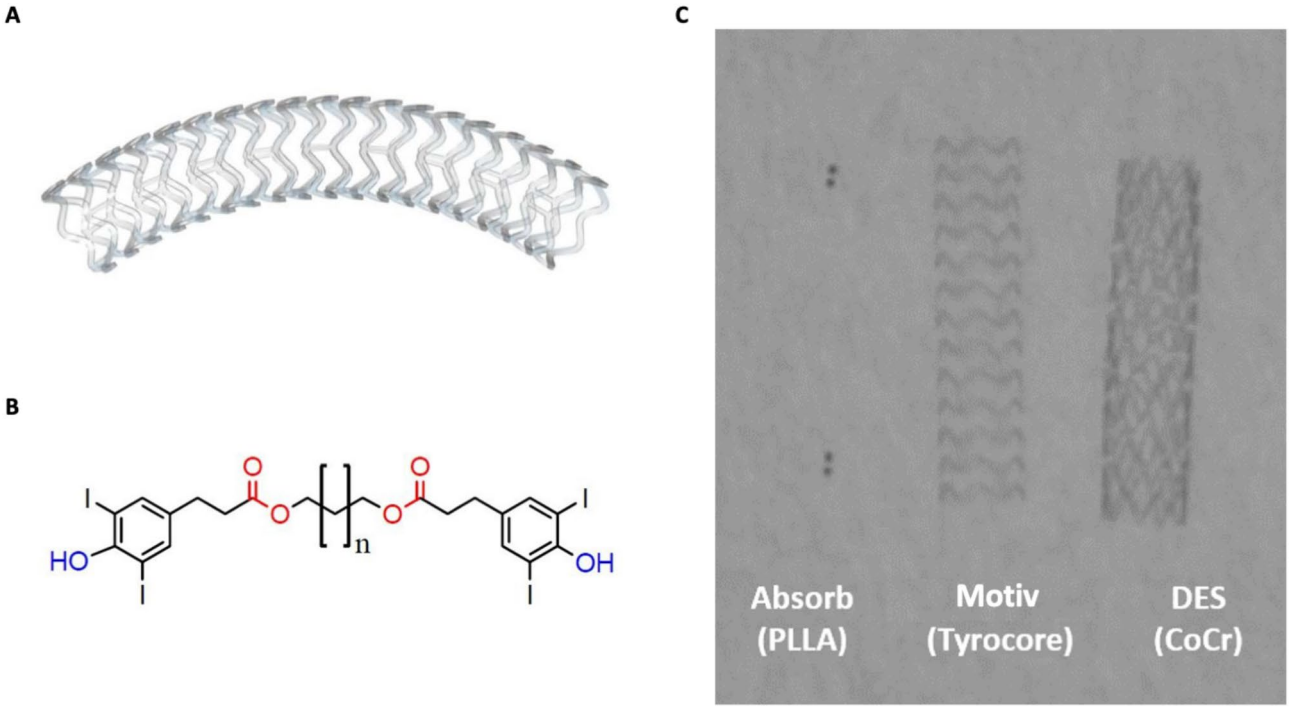

Fig. 1. (**A**) Open-cell scaffold design; (**B**) The polymer consists of two subunits - an iodinated diphenol and a low molecular weight oligomer of polylactic acid diol; (C) Direct visualization of the entire device under standard fluoroscopy.

Cohort / Group	Cohort / Group Description	Animal No.	Implant Site	Device Size
1	30 Day	1	RII	3.5 × 60 mm*
			LII	3.0 × 24 mm
		2	RII distal	3.5 × 12 mm
			RII proximal	3.5 × 12 mm
			LII	3.5 × 36 mm
		3	LII	3.0 × 36 mm*
			RII	3.0 × 48 mm
2	90 Day	4	LII	3.5 × 45 mm
		5	RII	3.5 × 60 mm
			LII distal	2.5 × 24 mm*
			LII proximal	3.0 × 36 mm*
		6	LII distal	3.0 × 12 mm
			LII proximal	3.5 × 12 mm
		7	LII	3.5 × 60 mm
			RII	3.5 × 48 mm*
		8	RII	3.0 × 48 mm
			LII distal	3.0 × 24 mm
			LII proximal	3.0 × 18 mm
		9	LII	3.0 × 18 mm
			RII	3.5 × 60 mm*

Table 1. Distribution of scaffolds among groups and arterial locations. RII = right internal iliac; LII = left internal iliac. *Vessels designated for SEM and not included in OCT substudy.

among animals and time points is presented in Table 1. Scaffolds were implanted with a targeted balloon-to-artery ratio of 1.1:1 into the iliac arteries using online Quantitative Vascular Angiography (QVA). Optical Coherence Tomography (OCT) imaging was performed post-implantation to confirm good apposition to the arterial wall. In absence of endovascular imaging-guided sizing, 9/20 scaffolds appeared undersized in post-

implant OCT and were post-dilated to optimize apposition. Group 1 and 2 animals underwent OCT imaging on all implanted vessels at post-implant and termination, excluding the ones designated for Scanning Electron Microscopy (SEM) (5 vessels in total, two (2) from Group 1 and three (3) from Group 2). Following termination (euthanasia was performed under general anesthesia with the use of pentobarbital sodium and phenytoin sodium solution) vessels containing the scaffolds were subjected to histology analysis.

OCT analysis

OCT pullbacks were performed at baseline (post-implant) and pre-termination at 30 and 90 days using Abbott's ILUMIEN OPTIS system and the Dragonfly™ Duo catheter. Images were analyzed by an in-house core laboratory (CRF Skirball Center for Innovation, Orangeburg, NY) using commercial software (ILUMIEN OPTIS, Abbott, Santa Clara, CA). Lumen area and the inner and outer scaffold areas, and corresponding diameters were measured planimetrically after calibration. Percentage area of stenosis (% AS), neointimal area (NA) and neointimal thickness (NIT) were derived from these measurements. The %AS was calculated according to the formula: %AS = (neointimal area/inner scaffold area) x100%. Neointimal area was calculated as inner scaffold area – lumen area. Neointimal thickness was calculated as inner scaffold diameter – lumen diameter.

The ratio of uncovered struts (ROUS) refers to the ratio of uncovered struts to the total number of struts. Covered struts were defined as having ≥ 20 μm of neointima over the strut. A ratio of covered struts ≥ 95% was considered acceptable for all devices. Late structural strut discontinuity was assigned if either of these two conditions existed: (1) two struts overhung each other in the same angular sector of the lumen perimeter, with or without malapposition, covered or uncovered; or (2) there was an isolated, covered or uncovered strut(s) located more or less at the center of the vessel, without obvious connection with other surrounding struts in OCT. Scaffold fracture was assumed in the case of overriding contiguous struts, disconnection from the expected device circularity, and isolated struts lying in the lumen. Malapposition refers to a strut that is not in contact with the artery wall. Malapposition was considered when the axial distance between the strut's surface and the luminal surface exceeded the strut thickness (95 μm for 2.5 mm; 105 μm for 3.0 mm; 115 μm for 3.5 mm scaffold). A strut that appeared non-apposed in the side branch regions, which often have geometry distortion, was excluded from the analysis. Malapposition distance, location, the total number of malapposed struts for the device, and averages for each group were reported. Of note, the OCT properties of the Tyrocore polymer are remarkably different from those of PLLA scaffolds; the abluminal surface of the strut is strongly reflective of light, resulting in a single line resembling a metallic strut reflection. As such, the visualization of the entire strut (and scaffold) footprint in the "box" form previously characterized for the PLLA scaffolds is not possible.

Histological preparation

All peripheral arteries implanted with the scaffolds were collected and perfusion-fixed with 10% NBF. The scaffolded arterial segments, as well as proximal and distal reference regions were processed and embedded in SPURR media, sectioned at three levels: proximal, middle, and distal, and stained with hematoxylin and eosin (H&E) and elastin trichrome (ET).

Scanning electron microscopy (SEM) preparation

The scaffold-containing coronary arteries designated for SEM were fixed en-bloc and later trimmed into two longitudinal sections. Each long section was processed and mounted onto an SEM stub for imaging. Digital SEM imaging was performed using a JEOL JSM-6610 microscope.

Arterial histomorphometry

Photomicrographs of histological ET-stained sections were measured with computer-assist software (Image-Pro® Plus 7). Measurements included the cross-sectional areas for external elastic lamina (EEL), internal elastic lamina (IEL), percent area stenosis (%), average neointima thickness (μm), neointimal area (NA, mm^2), and medial area (MA, mm^2). The derivative parameters were calculated as follows: percent area stenosis (based on internal elastic lamina area - IELA) = (1 – LA/IELA) × 100; average neointima thickness (μm) = (IELD-LD)/2 × 1000; neointimal area (NA, mm^2) = IELA-LA; medial area (MA, mm^2) = EELA – IELA.

Histological analysis

Blinded analysis of all slides was performed via light microscopy. Slides were evaluated for standard healing parameters, such as injury, endothelialization, inflammation, multinucleated giant cells, residual red blood cell distribution, fibrin, neovascular buds, medial necrosis/hemorrhage/fibrosis, adventitial/perivascular inflammation (severity and distribution) and assessed semi-quantitatively. Other factors analyzed included neointimal maturity, strut-associated calcification, adventitial fibrosis and presence of granulomas. All parameters were interpreted from the H&E and ET-stained slides. Per the consensus document for Drug-Eluting Stents in Preclinical Studies[21], it is recognized that granulomata occur regularly (typically less than 10% of vessels treated in a study) and vessels affected may be excluded from the analysis.

SEM analysis

All luminal regions of each treated vessel were evaluated for endothelial coverage and maturity, thrombus formation, and the presence of inflammatory cells and platelets. Endothelialization coverage and maturity were evaluated over and between struts if an outline of the struts underlying the neointima was visible. Proximal and distal hosts (non-treated segments) were also examined. The evaluation of healing was assessed from images at 50x, 100x, and 250x magnifications. Electron micrographs taken at other magnifications were evaluated if

provided. Non-parametric SEM features were scored between 0 and 4 (endothelialization, thrombus, leukocytes, platelets) with scores at or near zero denoting within the normal limits state.

Statistical analysis

For parametric variables, means ± SD were calculated for each group and assessed with Student t test, or analysis of variance and correction for multiple comparisons. Dichotomous variables such as injury score, endothelialization, and inflammation cannot be averaged but were presented categorically as mean ± SD. Numerical scores from the grading scale were converted to a percentage ranging from 0 to 100%.

Results

All animals (9) were successfully implanted and survived to 30 or 90 days. There were no adverse events reported on treatment day, nor during the observation period.

OCT

Following deployment of the devices, OCT was performed on 14 MOTIV scaffolds in 9 animals (no OCT analysis was performed on the SEM cases). An average overstretch ratio of 1.05 ± 0.07 was achieved for Group 1 animals, and 1.02 ± 0.06 for Group 2 animals based on OCT calculations post-implant. Following post-dilation where it was deemed necessary as described in Methods, no evidence of inadequate deployment nor malapposition was observed in the final post-deployment OCT.

At termination, all treated segments featured satisfactory patency (Figs. 2 and 3). The average neointimal thickness was 0.21 ± 0.05 mm in Group 1 (30 days) and 0.18 ± 0.10 mm in Group 2 (90 days)($p = 0.39$); the percent area stenosis (PAS) was 28 ± 7% in Group 1 and 24 ± 11% in Group 2 ($p = 0.35$); the neointimal area was 1.7 ± 0.35 and 1.42 ± 0.73 ($p = 0.33$) respectively. The neointimal area, thickness, and PAS between the two groups were comparable ($p > 0.050$). The outer scaffold area did not differ statistically among time points (Group 1 vs. Group 2–7.82 ± 0.51 vs. 7.52 ± 0.97, $p = 0.51$ at baseline; 7.23 ± 0.46 vs. 7.05 ± 0.99, $p = 0.69$ at termination). All struts examined were fully covered by neointima in both Groups. An average total of 56 ± 8 struts were counted in Group 1 and the ratio of uncovered struts (ROUS) was 0%; no malapposition, stent fracture, or late strut discontinuity was observed. The satisfactory structural integrity was also confirmed by post-mortem Faxitron imaging (Fig. 3). An average total of 52 ± 5 struts were counted in Group 2 and the ROUS was 0%; no malapposition, stent fracture, or late strut discontinuity was observed. The detailed OCT results are summarized in Table 2.

SEM

SEM analysis of two (2) MOTIV-treated vessels after 30 days demonstrated complete endothelialization (score 4) with no noteworthy platelet, red blood cell, or leukocyte adhesion, no fibrin deposition, and no unresorbed surface thrombus (all score 0). Minor surface artifacts (e.g., dehydration cracking along a strut), as well as endothelial erosion, were occasionally observed. SEM analysis of three (3) MOTIV-treated vessels after 90 days demonstrated complete endothelialization (score 4) with no noteworthy platelet (mostly 0) or leukocyte adhesion, no fibrin deposition, and no thrombosis (all score 0) (Fig. 4). One animal consistently demonstrated

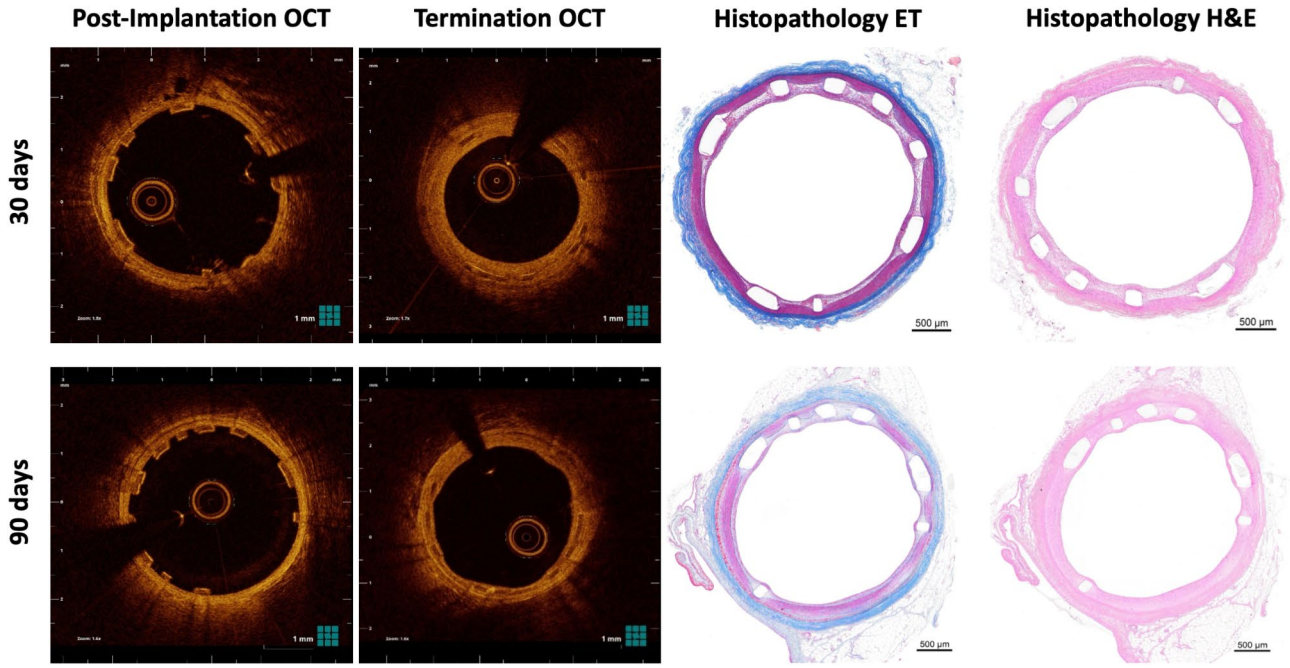

Fig. 2. Representative OCT and histopathology images of Motiv treated vessels at 30 and 90-day time point.

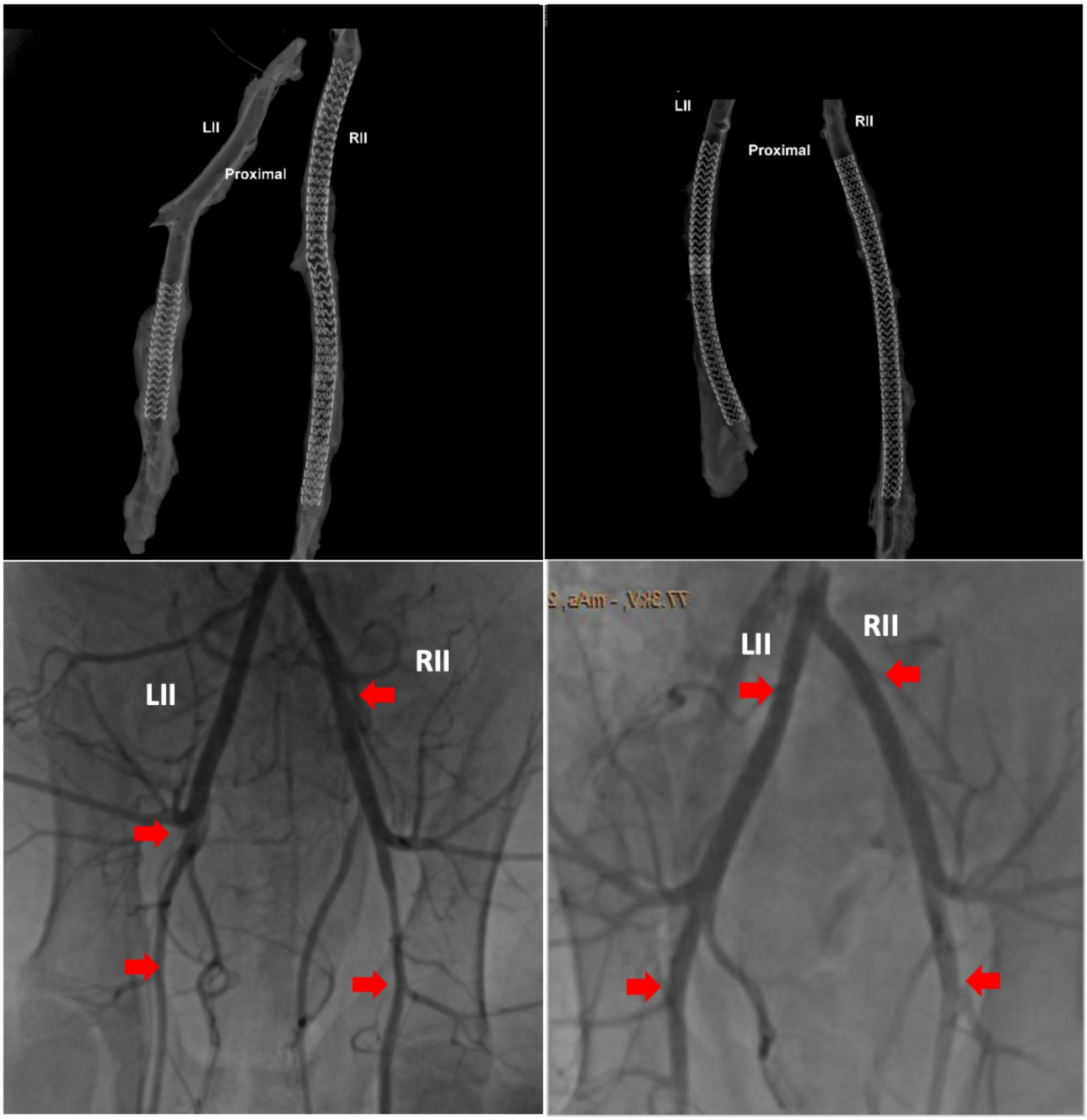

Fig. 3. RII = right internal iliac artery; LII = left internal iliac artery. Upper panels show post-mortem Faxitron images of scaffolds retrieved from two 90-day animals, showing adequately retained scaffold structure and integrity. Lower panels show corresponding pre-terminal (90-day) angiograms of the same arterial segments, demonstrating satisfactory patency. Red arrows indicate scaffold edges.

what was interpreted to be terminal endothelial erosion/denudation artifact and red blood cell pooling. Minor surface artifacts (e.g., surface cracking or peeling) were also occasionally observed. The polymer degradation/resorption was not observed in SEM analysis.

Histopathology

Vessel injury

At 30 days the average in-stent injury score was low, indicating a good apposition of the struts to the internal elastic lamina. There were only focal struts that penetrated IEL and were contacting the media, typically within a single quadrant. The 90-day cohort expressed similar results confirming a proper scaffold apposition in all but one vessel that demonstrated severe injury (stent strut penetrating the IEL, media, and EEL) at multiple struts/within multiple quadrants at every stented level. This injury was associated with extensive eosinophilic-rich

		Average Reference		Average In-Stent Segments								
		Distal reference lumen area	Distal reference lumen diameter	Lumen area	Lumen diameter	Scaffold (inner) area	Scaffold (inner) diameter	Scaffold (outer) area	Scaffold (outer) diameter	Neointimal Thickness	Neointimal Area	PAS*
		mm^2	mm	mm^2	mm	mm^2	mm	mm^2	mm	mm	mm^2	%
30-day Group	Post-implant	7.17	3.01	6.9	2.96	6.9	2.96	7.82	3.15	NA	NA	NA
		0.99	0.21	0.43	0.09	0.43	0.09	0.51	0.1	NA	NA	NA
	Term	6.34	2.82	4.36	2.35	6.06	2.77	7.23	3.03	0.22	1.7	28%
		0.99	0.21	0.53	0.14	0.38	0.09	0.46	0.1	0.05	0.35	6%
90-day Group	Post- implant	7.22	3.02	6.57	2.88	6.57	2.88	7.52	3.09	NA	NA	NA
		0.85	0.17	0.9	0.2	0.9	0.2	0.97	0.2	NA	NA	NA
	Term	7.52	3.07	4.6	2.4	6.02	2.76	7.05	2.98	0.18	1.42	24%
		1.55	0.31	1.09	0.28	0.92	0.21	0.99	0.21	0.1	0.73	11%

Table 2. Summary of OCT Results.

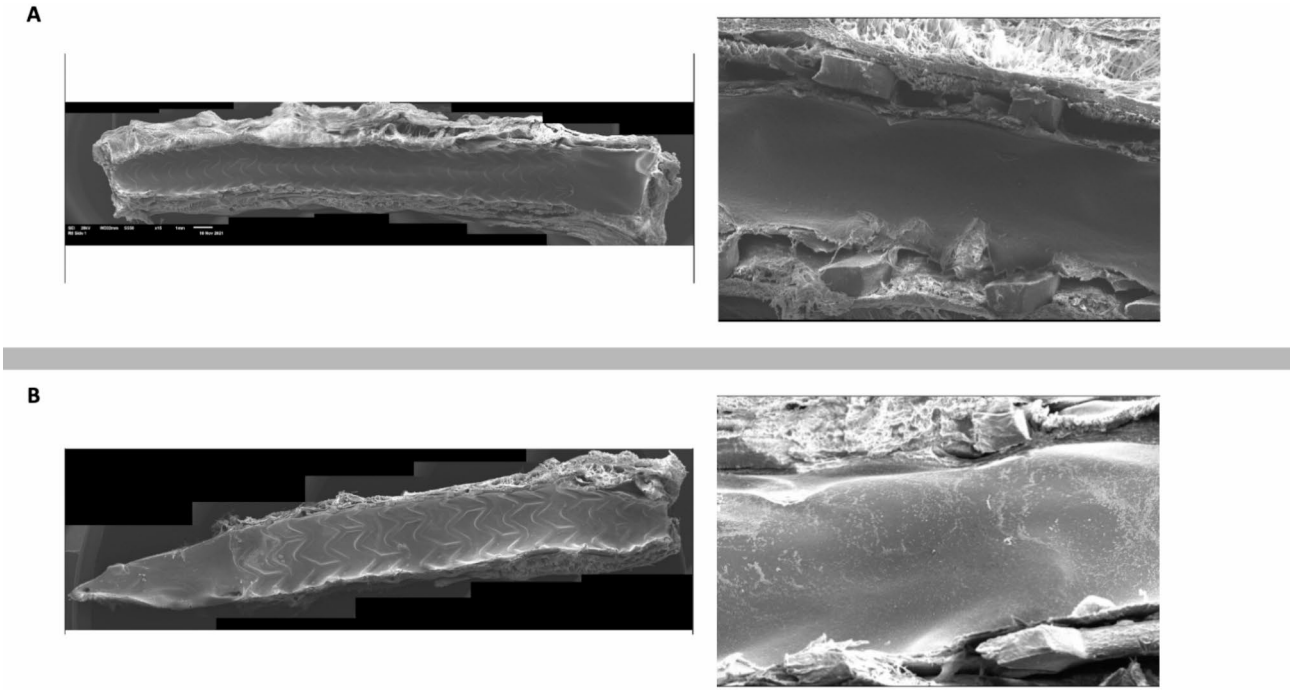

Fig. 4. Representative SEM images of Motiv treated vessels at 30 (**A**) and 90-day (**B**) time point.

granulomatous inflammation. The distal stented level had the least overall injury of the examined levels and demonstrated severe injury and accompanying inflammation around ~ 50% of the vessel circumference, with the remaining struts showing no to minimal injury, as well as minimal inflammation (Table 3).

Vessel healing

Adequate vessel wall healing at both time points was characterized by a typically fully mature neointima and complete reendothelialization at all sites. At 30 days, minimal to moderate fibrin deposition was observed adjacent to the struts and was overall decreased at 90 days with minimal fibrin deposition occasionally observed. No unresorbed luminal thrombus was observed in any vessel (Table 3).

Biological response to the scaffold

Overall, the inflammation scores were low for all vessels (characterized by minimal lymphocytes, macrophages, and multinucleated giant cells) on both time points except for one animal. The average inflammation (excluding multinucleated giant cells [MNGCs]) was 0.6 for the stented vessel segments at 30 days and was characterized by minimal scattered lymphocytes and macrophages (average MNGCs score was 0.9). As for the 90 days cohort, the inflammation scores were generally low with an average inflammation (excluding MNGCs) of 0.8 for the stented segments, characterized by minimal scattered lymphocytes and macrophages (average MNGCs score was 1.0) (Fig. 5; Table 3). In one animal from 90-day cohort the inflammation was defined by typically confluent or circumferential granulomatous formation, characterized by many granulocytes (predominately eosinophils but with many neutrophils) and macrophages, with fewer multinucleated giant cells and lymphocytes. These eosinophil-rich granulomas were observed adjacent to all struts at the proximal and mid-stented levels and were adjacent to half of the struts within the distal level.

At every level, this inflammation was associated with moderate to severe injury in which the strut penetrated the IEL and media and contacted or penetrated the EEL. Extension of inflammation into the adventitia was also observed at every level and was moderate in severity, affecting up to 25% (distal level) or up to 50% (proximal and mid-levels) of the adventitial circumference .

Quantitative histomorphometric evaluation

All vessels remain patent at all examined levels at both time points. The average percent area stenosis for the stented segments was 31% (20–36) and 35% (20–57) for 30- and 90-day respectively. One animal from Group 2 demonstrated the highest EEL area and the highest neointimal area, and thus increased percent area stenosis by 57% (Table 4).

Discussion

The MOTIV DRS is a novel scaffold designed for the treatment of below-the-knee lesions, characterized by its thin struts, rapid and broad expansion capability, and most uniquely, its radiopacity. The study aimed to evaluate the safety and performance of the MOTIV DRS in the porcine peripheral arteries model.

			Histologic Assessment														
			Vessel Wall Injury	Vessel Healing and Patency										Device Biocompatibility			
			Mean Injury	Endothelialization	Endothelial Erosion	Thrombosis	Fibrin	Neointima Maturity	Medial Necrosis/Hemorrhage	Medial Fibrosis	Adventitia Fibrosis	Neovascular Buds/Vascular	Calcification	Inflammation (excluding MNGC)	Multinucleated Giant Cells (MNGC)	Granuloma Formation	Adventitial/ Perivascular Inflammation
Scaffolded Section	30 Days	Mean	1.3	0	NA	0	2.1	0.1	0	0.3	0	0	0.3	0.6	0.9	NA	0.2
		SD	0.2	0	NA	0	0.6	0.3	0	0.5	0	0	0.5	0.5	0.3	NA	0.4
	90 Days	Mean	1.8	0	NA	0	0.7	0	0	0.8	0.8	0	0.2	1.1	1	NA	0.6
		SD	0.8	0	NA	0	0.4	0	0	0.7	0.7	0	0.4	0.9	0	NA	1.2
Reference Section	30 Days	Mean	0	0	NA	0	0	0	0	0	0	0	0	0	0	NA	0
		SD	0	0	NA	0	0	0	0	0	0	0	0	0	0	NA	0
	90 Days	Mean	0	0	NA	0	0	0.3	0	0	0	0	0	0	0	NA	0
		SD	0	0	NA	0	0	0.5	0	0	0	0	0	0	0	NA	0

Table 3. Semiquantitative assessment of key histologic outcomes. 0 = Not present; 1 = Present, but minimal feature; 2 = Notable feature, mild; 3 = Prominent feature that does not disrupt tissue architecture and is not overwhelming, moderate; 4 = Overwhelming feature or feature that effaces or disrupts tissue architecture, marked or severe.

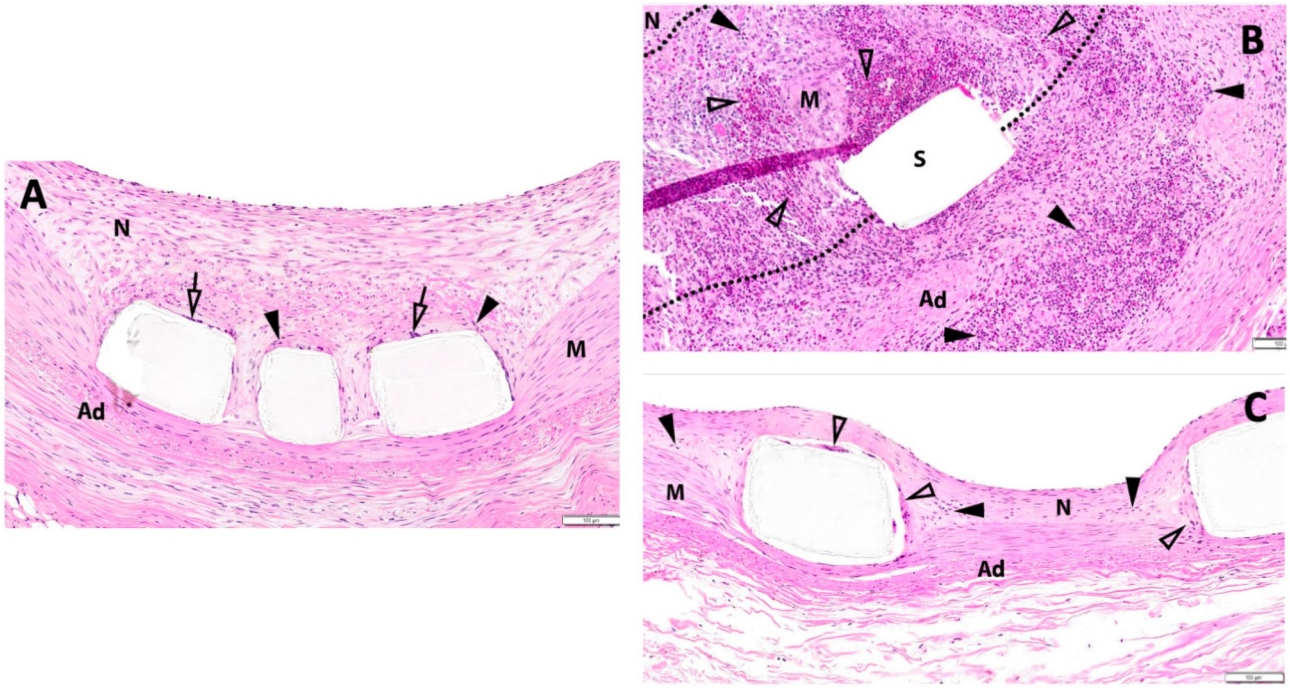

Fig. 5. (**A**) 30 Days. Minimal inflammatory aggregates characterized by scattered lymphocytes and macrophages (black arrowheads) and multinucleated giant cells (clear arrows) adjacent to the strut; N = neointima; M = media; Ad = adventitia; (**B**) 90 Days. Strut (S) associated granulomatous response characterized by many eosinophils (clear arrowheads), neutrophils (black arrowheads), and macrophages with rare multinucleated giant cells. Inflammation was associated with destruction of the IEL, EEL, and expansion of the adventitia; dotted lines = approximate demarcation of vessel neointima (N), media (M) and adventitia (Ad); (**C**) 90 Days. Minimal inflammatory aggregates characterized by scattered macrophages and lymphocytes (black arrowheads) and multinucleated giant cells (clear arrowheads) adjacent to the strut; N = neointima; M = media; Ad = adventitia.

Intravascular imaging confirmed that all scaffolds maintained their device integrity by showing no notable malapposition, fracture, or late strut discontinuity at 30- or 90-days post-termination in the stented internal iliac arteries. All struts were fully covered/embedded at both time points and the vessels remain patent. The measured percent area stenosis was comparable between groups. The average values of 28 ± 6% (30 days) and 24 ± 11% (90 days) respectively are acceptable and comparable with numbers presented for the drug-eluting stents tested in porcine peripheral arteries[22,23]. These findings were corroborated by histomorphometry revealing comparable percent area stenosis values except for one vessel that demonstrated the greatest EEL area and greatest neointimal area. This indicates that the intense inflammatory response noted in that vessel was associated with both positive vessel wall remodeling with expansion of the EEL area, as well as neointimal hyperplasia (and thus increased percent area stenosis – 57%).

Overall, almost all tested devices showed a very good biocompatibility that was indicated by the low inflammation scores, reflecting minimal infiltration of lymphocytes, macrophages, and multinucleated giant cells. Nevertheless, in one animal mentioned above, an excessive reaction in the form of granulomatous inflammation was described. Similar findings were previously reported and are known to occur regularly in swine and are considered to represent a type IV hypersensitivity reaction[21]. It is also recognized that in humans, late stent thrombosis in sirolimus-eluting stents has been attributed to a similar hypersensitivity reaction[24]. Recent studies suggest biodegradable/bioresorbable-coated polymers may result in reduced late inflammatory reactions and overall better outcomes compared to permanent polymers or bare metal stents but note that different polymer coatings and any significance to clinical use in humans remain to be elucidated[25]. This animal may therefore represent an individual 'reactor' demonstrating pig-to-pig variability in immune responsiveness.

Microscopic evaluation confirmed a low injury caused by implanted scaffolds. The struts were well apposed and rarely penetrated through the intima to more external layers. At both time points the stents were fully covered with typically fully mature neointima indicating a good vessel wall healing. The described fibrin deposits were minimal to moderate at 30 days' time point and decreased over time being occasionally observed at longer follow-up. Fibrin is considered a surrogate biomarker for the presence of an anti-proliferative drug[26] since delayed healing is an inevitable consequence of pharmacologic containment of neointimal proliferation with the agent eluted from the scaffold surface. Fibrin deposits have been shown to peak at 1-month post-implant for the Absorb scaffolds in the porcine coronary artery model[26]. MOTIV scaffolds exhibited rather scarce fibrin deposits. This would be a desirable finding as long as it does not occur at the price of decreased anti-restenotic efficacy. However, it does not seem to be the case for the scaffold in the present study, as it demonstrated adequate

		Morphometry Assessment										
		Area Measurements (mm^2)					Length Measurements (mm)			Restenosis Parameters		
		EEL Area	IEL Area	Lumen Area	Medial Area	Neointimal Area	Lumen Perimeter	Lumen equivalent Diameter	IEL Equivalent Diameter	Average Neointima Thickness (µm)	Percent Area Stenosis (%)	
Scaffolded section	30 Days	5.88	5.09	3.55	0.78	1.54	7.03	2.08	2.5	210.42	31%	Mean
		1.91	1.65	1.28	0.28	0.58	1.5	0.46	0.5	60.6	7%	SD
	90 Days	6.79	5.9	3.75	0.88	2.15	7.37	2.17	2.73	284	35%	Mean
		0.98	0.85	0.98	0.2	1.24	1.04	0.29	0.19	169.93	16%	SD
Reference section	30 Days	5.63	4.68	4.2	0.95	0.48	7.4	2.26	2.39	62.5	9%	Mean
		2.01	1.78	1.73	0.28	0.82	1.51	0.47	0.49	108.25	15%	SD
	90 Days	4.15	3.14	3.11	1.01	0.03	6.32	1.98	1.99	4.38	1%	Mean
		0.7	0.58	0.56	0.24	0.03	0.72	0.18	0.18	5.27	1%	SD

Table 4. Quantitative histomorphometric results.

containment of neointimal response, comparable to the ones reported in other preclinical studies, even with drug-eluting stents[22,23].

SEM data provide the most reliable assessment of endothelial coverage of the stented segment of a peripheral artery. SEM analysis relies upon *en-face* views with suitable magnifications of the entire luminal surface of a bisected vessel, which is more comprehensive than light microscopic evaluations commonly performed on limited numbers of transverse sections ($n = 3$) per treated vessel. At 1 and 3 months, the MOTIV-treated vessels exhibited complete endothelial coverage over and between struts with, in general, no noteworthy findings observed (such as thrombosis, fibrin deposition, platelet adhesion, etc.). Minor surface artifacts and endothelial erosion were occasionally described. They can be attributed to the device preparation (dehydration cracking along a strut) and/or terminal angiography performed and are a common finding when utilizing so accurate and high-resolution modality. However, one animal consistently demonstrated what was interpreted to be terminal endothelial erosion/denudation artifact and red blood cell pooling. These findings can be attributed to the excessive and abnormal inflammatory reaction reported in this animal as described earlier.

The positive preclinical findings of the tested scaffold may not be directly translated to the clinical setting owing to the lack of atherosclerotic disease in animals and thus should be interpreted with caution. Nevertheless, they constitute a valuable source of information helping to understand the associated healing process and uncover any potential threats, knowing the shortcomings of the first generation PLLA scaffolds. The described good safety and biocompatibility profile of MOTIV stents is in line with recently presented results of a multicenter study in BTK lesions demonstrating improvement in Rutherford Classification and wound healing (58 patients, 60 study limbs, and 76 Motiv scaffolds) at 24 months (81.7% of stents were patent with a limb salvage rate amounting to 95%)[17].

The Tyrocore-made scaffolds (MOTIV, Fantom) were designed to overcome the limitations of first-generation PLLA DRS. For instance, the literature suggests an unfavorable peristrut rheology for first-generation thick-strut DRS, as compared with metallic stents[27,28]. Low shear stress regions and altered flow patterns in between Absorb struts were identified by three-dimensional angiographic reconstruction techniques and computational fluid dynamic data[29]. Low endothelial shear stress has been long recognized as a powerful local stimulus for atherogenesis, formation, and progression of an early atherosclerotic plaque to high-risk plaque[30]. Lastly, an ex-vivo porcine arteriovenous shunt model and a rabbit model of iliofemoral stent implantation demonstrated increased thrombogenicity quantified by platelet aggregation and inflammatory cell adhesion in Absorb when compared to thin strut biodegradable polymer coated DES[31]. The evidence summarized above suggests the key role of lowering strut thickness without loss of radial strength to further improve DRS technology[32]. The struts of MOTIV scaffolds are around 27–39% (dependent on the scaffold size) thinner than the ones of Absorb (95–115 μm vs. 157 μm).

Interestingly, despite the disappointing long-term results of first-generation PLLA scaffolds in coronary arteries, the reported long-term outcomes of ABSORB BTK showed primary patency (defined as freedom from peak systolic velocity ratio > 2.0 or target vessel occlusion) and freedom from clinically driven target lesion revascularization rates of 89.2%/80.3%/72.9% and 97.2%/90.7%/90.7% at 12, 36, and 60 months, respectively. The authors reported no late or very late scaffold thrombosis[16]. Even more important, the recently published results of multicenter Life BTK RCT (261 patients with CLTI) comparing the Esprit scaffold (thin strutted Absorb) against angioplasty (randomized in a 2:1 ratio) showed that the DRS constitutes a viable treatment alternative[18].

The accumulating preclinical and clinical data suggest that the BTK arteries might be an appropriate target for bioresorbable technologies. Combined with the proper implantation and vessel preparation technique, such as PSP (predilation, sizing, and post-dilation) achieving positive long-term results was possible even with the discontinued first-generation scaffolds. On this background, gradual improvement on the shortcomings of the early technologies has allowed progress with current generation of devices for this very challenging arterial territory.

Limitations

Some study limitations must be acknowledged. The relatively small number of animals and devices evaluated should be considered when interpreting the results. The 30- and 90-day interim data do provide a snapshot of the healing profile and have been previously accepted as sufficient preliminary preclinical evidence for novel DRS[33,34], but the follow-up of 3 months is now considered quite short for animal studies of DRS given the multi-year degradation process and the delayed nature of adverse clinical sequelae identified for Absorb. However, it needs to be emphasized that an earlier generation coronary device - the Fantom scaffold, made of a similar tyrosine-based polymer, was previously studied preclinically out to 4 years revealing no concerns[35]. Additionally, recently presented 5-year clinical outcomes of the FANTOM II study corroborated the long-term device safety with MACE rate, target lesion failure, and scaffold thrombosis reported in 6.3%, 5.8%, and 1.3% patients respectively[14]. Furthermore, as described previously, MOTIV scaffolds identical to the one studied in the present study demonstrated a favorable 24-month clinical safety profile and angiographic results[17]. Secondly, although the porcine peripheral arteries model is a well-established and desired one[21], the implantation of scaffolds in native vessels of young animals without atherosclerotic disease may limit the ability to directly translate the preclinical results to clinical settings. However, the previously mentioned clinical data do support our findings.

Conclusion

Implantation of the MOTIV DRS up to 60 mm long in small-caliber peripheral arteries of swine resulted in 100% patency rate and adequate vascular healing at 30-day and 90-day timepoints. The Tyrocore-based DRS retained their integrity and radial strength throughout the course of the study and confirmed their favorable biocompatibility in small-caliber porcine peripheral arteries thus confirming the study hypothesis. The scaffolds retained their necessary structural integrity (and thus also, presumably, sufficient radial strength) throughout

the course of the study and confirmed their safety in the preclinical setting. Combined with positive clinical results, the MOTIV DRS has a chance to constitute an alternative for the treatment of below-the-knee lesions, adding to currently limited interventional armamentarium.

Data availability

The data is presented within the manuscript. The raw data that support the findings of this study can be available from the corresponding author upon reasonable request and with permission from REVA Medical LLC.

Received: 26 September 2024; Accepted: 24 February 2025
Published online: 27 March 2025

References

1. Fowkes, F. G. et al. Comparison of global estimates of prevalence and risk factors for peripheral artery disease in 2000 and 2010: a systematic review and analysis. *Lancet* **382**, 1329–1340. https://doi.org/10.1016/S0140-6736(13)61249-0 (2013).
2. Nehler, M. R. et al. Epidemiology of peripheral arterial disease and critical limb ischemia in an insured national population. *J. Vasc. Surg.* **60**, 686–695e2. https://doi.org/10.1016/j.jvs.2014.03.290 (2014).
3. Conte, M. S. et al. Global vascular guidelines on the management of chronic limb-threatening ischemia. *J. Vasc. Surg.* **69**(6S):3S–125S.e40. https://doi.org/10.1016/j.jvs.2019.02.016 (2019).
4. Liu, X., Zheng, G. & Wen, S. Drug-eluting stents versus control therapy in the infrapopliteal disease: A meta-analysis of eight randomized controlled trials and two cohort studies. *Int. J. Surg.* **44**, 166–175. https://doi.org/10.1016/j.ijsu.2017.06.075 (2017).
5. Varcoe, R. L., Paravastu, S. C., Thomas, S. D. & Bennett, M. H. The use of drug-eluting stents in infrapopliteal arteries: an updated systematic review and meta-analysis of randomized trials. *Int. Angiol.* **38**, 121–135. https://doi.org/10.23736/S0392-9590.19.04049-5 (2019).
6. Rastan, A. et al. Sirolimus-eluting stents for treatment of infrapopliteal arteries reduce clinical event rate compared to bare-metal stents: long-term results from a randomized trial. *J. Am. Coll. Cardiol.* **60**, 587–591. https://doi.org/10.1016/j.jacc.2012.04.035 (2012).
7. Grewe, P. H., Deneke, T., Machraoui, A., Barmeyer, J. & Müller, K. M. Acute and chronic tissue response to coronary stent implantation: pathologic findings in human specimen. *J. Am. Coll. Cardiol.* **35**, 157–163. https://doi.org/10.1016/s0735-1097(99)00486-6 (2000).
8. Joner, M. et al. Pathology of drug-eluting stents in humans: delayed healing and late thrombotic risk. *J. Am. Coll. Cardiol.* **48**, 193–202. https://doi.org/10.1016/j.jacc.2006.03.042 (2006).
9. Karnabatidis, D. et al. Incidence, anatomical location, and clinical significance of compressions and fractures in infrapopliteal balloon-expandable metal stents. *J. Endovasc. Ther.* **16**, 15–22. https://doi.org/10.1583/08-2530.1 (2009).
10. Maeda, K. & Ohki, T. Endovascular therapeutic technique. In *Rutherford's Vascular Surgery and Endovascular Therapy* 9th edn (eds Sidawy, A. N. & Perler, B. A.) 762–784 (Elsevier, Philadelphia, 2019).
11. Wykrzykowska, J. J. et al. Bioresorbable scaffolds versus metallic stents in routine PCI. *N Engl. J. Med.* **376**, 2319–2328. https://doi.org/10.1056/NEJMoa1614954 (2017).
12. Serruys, P. W. et al. Comparison of an everolimus-eluting bioresorbable scaffold with an everolimus-eluting metallic stent for the treatment of coronary artery stenosis (ABSORB II): a 3 year, randomised, controlled, single-blind, multicentre clinical trial. *Lancet* **388**, 2479–2491. https://doi.org/10.1016/S0140-6736(16)32050-5 (2016).
13. Kaluza, G. L. & Granada, J. F. The bioresorbable vascular scaffold tale epilogue: overpromised, underdelivered, prematurely degraded. *JACC Cardiovasc. Interv.* **12**, 980–982 (2019).
14. Lutz, M. et al. Long-term safety and effectiveness of the Fantom bioresorbable coronary artery scaffold: final results of the FANTOM II trial. *EuroIntervention* **20**, e453–e456. https://doi.org/10.4244/EIJ-D-23-00504 (2024).
15. Pompei, G. et al. Long-term outcomes of patients treated with sirolimus-eluting resorbable magnesium scaffolds: insights from the SHERPA-MAGIC study. *Int. J. Cardiol.* **383**, 1–7 (2023).
16. Varcoe, R. L., Menting, T. P., Thomas, S. D. & Lennox, A. F. Long-term results of a prospective, single-arm evaluation of everolimus-eluting bioresorbable vascular scaffolds in infrapopliteal arteries. *Catheter Cardiovasc. Interv.* **97**, 142–149. https://doi.org/10.1002/ccd.29327 (2021).
17. Rand, T. MOTIV bioresorbable BTK scaffold pilot study. Initial 24 months results. Presented at Cardiovascular and Interventional Radiological Society of Europe (CIRSE) annual congress; September 9, 2023; Copenhagen, Denmark.
18. Varcoe, R. L. et al. Drug-Eluting resorbable scaffold versus angioplasty for infrapopliteal artery disease. *N. Engl. J. Med.* **390**, 9–19. https://doi.org/10.1056/NEJMoa2305637 (2023).
19. Brodmann, M. RESOLV FIH 6-month results by Rutherford classification. Presented at Vascular InterVentional Advances (VIVA) conference; October 31, 2023; Las Vegas, Nevada, USA.
20. Auras, R., Lim, L. T., Selke, S. & Tsuji, H. Poly(lactic acid): synthesis, structures, properties, processing, and applications. 1–1. https://doi.org/10.1002/9780470649848 (Wiley, 2010).
21. Schwartz, R. S. et al. Drug-eluting stents in preclinical studies: updated consensus recommendations for preclinical evaluation. *Circ. Cardiovasc. Interv.* **1**, 143–153. https://doi.org/10.1161/CIRCINTERVENTIONS.108.789974 (2008).
22. Sakamoto, A. et al. Vascular response of a polymer-free paclitaxel-coated stent (Zilver PTX) versus a polymer-coated paclitaxel-eluting stent (Eluvia) in healthy swine femoropopliteal arteries. *J. Vasc Interv Radiol.* **32** (6), 792–801e5. https://doi.org/10.1016/j.jvir.2021.02.014 (2021).
23. Gasior, P. et al. Impact of fluoropolymer-based paclitaxel delivery on neointimal proliferation and vascular healing: A comparative peripheral drug-eluting stent study in the familial hypercholesterolemic swine model of femoral restenosis. *Circ. Cardiovasc. Interv.* **10** (5), e004450. https://doi.org/10.1161/CIRCINTERVENTIONS.116.004450 (2017).
24. Wilson, G. J. et al. Comparison of inflammatory response after implantation of sirolimus-and paclitaxel-eluting stents in porcine coronary arteries. *Circulation* **120**, 141–142. https://doi.org/10.1161/CIRCULATIONAHA.107.730010 (2009).
25. Ijichi, T. et al. Late neointimal volume reduction is observed following biodegradable polymer-based drug eluting stent in porcine model. *Int. J. Cardiol. Heart Vasc.* **34**, 100792. https://doi.org/10.1016/j.ijcha.2021.100792 (2021).
26. Otsuka, F. et al. Long-term safety of an everolimus-eluting bioresorbable vascular scaffold and the cobalt-chromium XIENCE V stent in a porcine coronary artery model. *Circ. Cardiovasc. Interv.* **7**, 330–342. https://doi.org/10.1161/CIRCINTERVENTIONS.113.000990 (2014).
27. Tenekecioglu, E. et al. Preclinical assessment of the endothelial shear stress in porcine-based models following implantation of two different bioresorbable scaffolds: effect of scaffold design on the local haemodynamic micro-environment. *EuroIntervention* **12**, 1296. https://doi.org/10.4244/EIJY16M05_01 (2016).
28. Kumar, A. et al. Bioresorbable vascular scaffolds versus everolimus-eluting stents: a biomechanical analysis of the ABSORB III imaging substudy. *EuroIntervention* **16** (12), e989–e996. https://doi.org/10.4244/EIJ-D-19-01128 (2020).
29. Gogas, B. D. et al. Biomechanical assessment of fully bioresorbable devices. *JACC Cardiovasc. Interv.* **6**, 760–761. https://doi.org/10.1016/j.jcin.2013.04.008 (2013).

30. Chatzizisis, Y. S. et al. Role of endothelial shear stress in the natural history of coronary atherosclerosis and vascular remodeling: molecular, cellular, and vascular behavior. *J. Am. Coll. Cardiol.* **49**, 2379–2393. https://doi.org/10.1016/j.jacc.2007.02.059 (2007).
31. Koppara, T. et al. Thrombogenicity and early vascular healing response in metallic biodegradable polymer-based and fully bioabsorbable drug-eluting stents. *Circ. Cardiovasc. Interv.* **8**, e002427. https://doi.org/10.1161/CIRCINTERVENTIONS.115.002427 (2015).
32. Kang, J. et al. Bioresorbable vascular scaffolds - Are we facing a time of crisis or one of breakthrough? *Circ. J.* **81** (8), 1065–1074. https://doi.org/10.1253/circj.CJ-17-0152 (2017).
33. Durand, E. et al. Head-to-head comparison of a drug-free early programmed dismantling polylactic acid bioresorbable scaffold and a metallic stent in the porcine coronary artery: six-month angiography and optical coherence tomographic follow-up study. *Circ. Cardiovasc. Interv.* **7** (1), 70–79. https://doi.org/10.1161/CIRCINTERVENTIONS.113.000738 (2014).
34. Cheng, Y. et al. Comparative characterization of biomechanical behavior and healing profile of a novel ultra-high-molecular-weight amorphous poly-L-lactic acid sirolimus-eluting bioresorbable coronary scaffold. *Circ. Cardiovasc. Interv.* **9**, e004253. https://doi.org/10.1161/CIRCINTERVENTIONS.116.004253 (2016).
35. Strandberg, E., Zeltinger, J., Schulz, D. G. & Kaluza, G. L. Late positive remodeling and late lumen gain contribute to vascular restoration by a non-drug eluting bioresorbable scaffold: a four-year intravascular ultrasound study in normal porcine coronary arteries. *Circ. Cardiovasc. Interv.* **5**, 39–46. https://doi.org/10.1161/CIRCINTERVENTIONS.111.964270 (2012).

Author contributions

MK– conceptualization, writing – original draft, investigation; PHCM – visualization, writing – original draft, investigation; YC– data curation, formal analysis, visualization; GBC– data curation, formal analysis; DG– supervision, validation; JA– supervision, validation; SDR– data curation, formal analysis, visualization; SAP– supervision, methodology, writing – review and editing; JFG – supervision, methodology, writing – review and editing; GLK– conceptualization, writing – original draft, supervision.

Declarations

Competing interests

The study has been funded by the scientific grant from REVA Medical LLC. Danielle Gram BS, BA and Jeffrey Anderson BS are employees of REVA Medical LLC. No other authors have a conflict of interest.

Additional information

Correspondence and requests for materials should be addressed to G.L.K.

Reprints and permissions information is available at www.nature.com/reprints.

Publisher's note Springer Nature remains neutral with regard to jurisdictional claims in published maps and institutional affiliations.